Proceedings of the
International Conference on Mechanical Engineering and Renewable Energy 2017
(ICMERE2017) 18 – 20 December, 2017, Chittagong, Bangladesh

ICMERE2017-PI-129

NUMERICAL AND EXPERIMENTAL INVESTIGATION OF THE INFLUENCE OF SERRATED GURNEY FLAP OVER A NACA 2412 AIRFOIL

Sanjoy Kumar Saha[1,*] and Md. Mahbubul Alam[2]

[1-2]Department of Mechanical Engineering
Chittagong University of Engineering & Technology, Chittagong-4349, Bangladesh
[1]sanjoysaha.cuet@gmail.com, [2]mahbub87@yahoo.com

Abstract- *Gurney flap, a small flat plate at the suction side stabilizes the wake which ensures laminar flow and thus shifts the shock. This study investigated the aerodynamic effect of serrated Gurney flap on a NACA 2412 airfoil. This involves a three-dimensional numerical and a wind tunnel investigation of the effectiveness of Gurney flap. Flap height ranges from 2% to 5% C and the serration depth and width were 0.01C which came into two shapes; triangular and square. The performance test was conducted in low speed wind tunnel under subsonic Mach number. The numerical analysis was performed using CFD software to predict the flow field. The analysis shows that the serrations tend to increase lift to drag ratio significantly and square serration provides the best performance rather than triangular serrated flap. The investigation concludes with a suggestion that serrated Gurney flap may lead to drag reduction in high lift regions.*

Key words: Computational Fluid Dynamics, Serrated Gurney flap, Flow control**,** Aerodynamic characteristics, Lift enhancement.

1. INTRODUCTION

High-lift aerodynamics continues playing an important role in the design of new aircrafts with maximum utilization of fuel and technology available. An effective high-lift system is necessary in order to climb to the cruise altitude at take-off and to be able to fly at the necessary low maneuver speeds in case of landing. Aerodynamic stability and flight behavior of the modern aircrafts is manipulated using aileron, elevators or flap by controlling the airflow toward the wing. The trailing edge geometry exerts a great influence on the performance of the aircraft. The integration of the gurney flap at the trailing edge has been proved to be aerodynamically beneficial. It works by separating the air flow turning over the backside of the flap near the trailing edge. So, the pressure is decreased on the suction side and increased on the pressure side. This results in an increase in lift of the airfoil and a shift in the zero lift angle of attack [1] and pressure on airfoil surface. This reversed flow region is consists of two contra-rotating vortices which altered the Kutta condition and circulation in the region. (Figure. 01) This ensures an increment in lift force, slight reduction in drag, laminar flow on the suction side of the wing and thereby stabilizes wake. An increase in the lift to drag ratio makes it possible to attain cruise altitude faster and stepper take off as well as reduces the noises being imparted. The effectiveness of Gurney flap is dependent on the size of the flap and the location and on the ratio of the velocity of the flow on the upper surface to the mean velocity of the lower surface. [2]

(a) Conventional airfoil

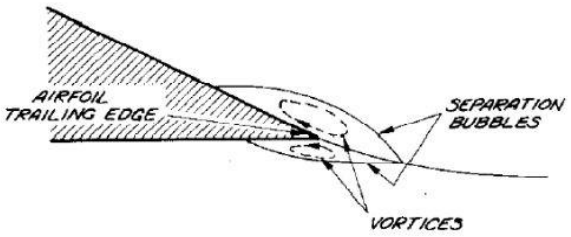

(b) Airfoil with a Gurney flap

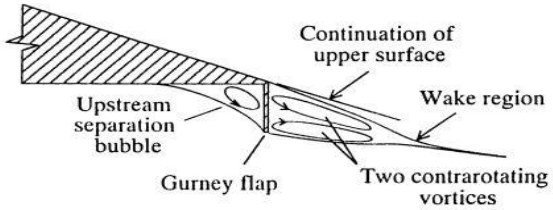

Fig.01: Hypothesized trailing edge flow structure for a (a) Conventional airfoil (b) airfoil with a Gurney flap [3]

The aerodynamic flow behavior can be investigated by means of numerical, analytical or experimental strategy.

Computational Fluid Dynamics (CFD) simulations are very common as well as an effective approach which is accompanied by means of proper mathematical model generally called as the governing equations. CFD is a computational technology that enables us to study things that flow and not only predicts fluid flow behavior, but also the heat transfer, mass, phase change, chemical reaction, mechanical movement and thermal stresses or deformation of related solid structures and electromagnetics as well as multiphysics.

2. INVESTIGATION APPROACH

2.1 Airfoil Selection:

Selecting an airfoil to study is a difficult task to perform. The NACA airfoils are airfoil shapes for aircraft wings developed by the National Advisory Committee for Aeronautics (NACA). In this investigation NACA 2412 was selected and scaled schematic of NACA 2412 is shown in figure 02. The airfoils are controlled by 4 digits which designate the camber, position of the maximum camber and thickness. For NACA 2412 airfoil model, camber is 0.02C; maximum camber is at 40%C and thickness is 0.12C.

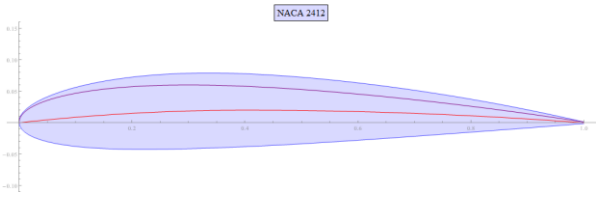

Fig.02: Scaled schematic of NACA 2412 airfoil. [4]

2.2 Numerical Method:

Computational Fluid Dynamics (CFD) refers to the solving a set of equations to predict the flow field of any investigation. Now-a-days CFD software is very widely used and a number of flexible commercial software is developed to study the fluid flow problems.

2.2.1 Governing Equations:

For this investigation, two equation turbulence model namely the k- ε model is used. This model is based on the fundamental concepts in physics of conservation of mass, momentum and energy along with two extra transport equations to represent the turbulent properties of the flow. [5]

The continuity equation is imprinted as:

$$\frac{\partial \rho}{\partial t} + \frac{\partial}{\partial x_j}(\rho U_j) = 0$$

The momentum equation is imprinted as:

$$\frac{\partial \rho U_i}{\partial t} + \frac{\partial}{\partial x_j}(\rho U_i U_j) = -\frac{\partial p}{\partial x_i} + \frac{\partial}{\partial x_j}\left[\mu_{eff}\left(\frac{\partial U_i}{\partial x_j} + \frac{\partial U_j}{\partial x_i}\right)\right] + S_M$$

Transport equations:

$$\frac{\partial}{\partial t}(\rho k) + \frac{\partial}{\partial x_j}(\rho k U_j) = \frac{\partial}{\partial x_j}\left[\left(\mu + \frac{\mu_t}{\sigma_k}\right)\frac{\partial k}{\partial x_j}\right] + P_k + P_b - \rho\epsilon - Y_M + S_k$$

$$\frac{\partial}{\partial t}(\rho\epsilon) + \frac{\partial}{\partial x_j}(\rho\epsilon U_j) = \frac{\partial}{\partial x_j}\left[\left(\mu + \frac{\mu_t}{\sigma_\epsilon}\right)\frac{\partial \epsilon}{\partial x_j}\right] + \rho C_1 S_\epsilon - \rho C_2 \frac{\epsilon^2}{k + \sqrt{\vartheta\epsilon}} + C_{1\epsilon}\frac{\epsilon}{k} C_{3\epsilon} p_b + S_\epsilon$$

Where,

$$C_1 = max\left[0.43, \frac{\eta}{\eta + 5}\right], \eta = S\frac{k}{\epsilon}, S = \sqrt{2S_{ij}S_{ij}}$$

Model constants are:

$$C_{1\epsilon} = 1.44,\ C_2 = 1.9,\quad \sigma_k = 1.0, \sigma_\epsilon = 1.2$$

In the above equations, P_k represents the generation of turbulence kinetic energy due to the mean velocity gradients, calculated in same manner as standard k- ε model. Here, P_b is the generation of turbulence kinetic energy due to buoyancy, calculated in same way as standard k-ε model.

2.2.2 CAD Model:

The three dimensional CAD model was built with SolidWorks using the 'Curves using XYZ point' function as shown in figure 03. Chord length was taken 200 mm and span was taken 120 mm for the convenience of using the airfoil in wind tunnel. This CAD model was fabricated for wind tunnel experiment and imported as external geometry file in CFD software.

(a) Rectangular serration

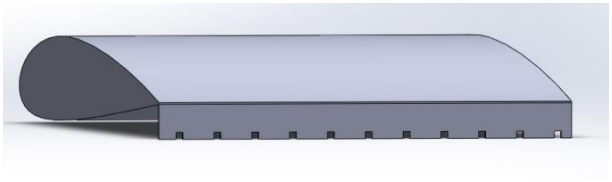

(b) Triangular serration

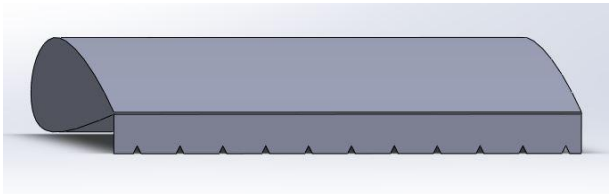

Fig.03: CAD model of NACA 2412 with serration

2.2.3 Mesh Generation:

The computational fluid domain is assumed to be made of solid air interface. The computational fluid domain consists of a semicircle and a rectangular shaped contour around the airfoil. A fine mesh results in higher number of calculations and thereby makes the simulation time longer. For this investigation, a structured triangular mesh was used. (Figure 04 and 05)

2.2.3 Boundary Conditions:

In this investigation, the software was run in an implicit pressure base, the simple pressure-velocity coupling for both the first and second order. The second order upwind scheme was used for higher accuracy. Wall boundary conditions were applied to the wind tunnel walls and the airfoil surface. A "velocity-inlet" condition was imposed for the inlet with a speed of 5m/s. The outlet was set to "pressure-outlet". For inflow turbulence, the

intensity and viscosity ratio specification method was specified with a turbulence intensity of 1%.

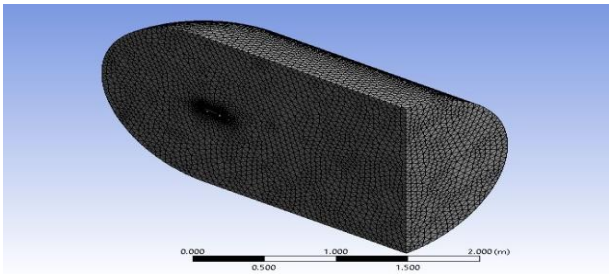

Fig. 04: Generation of mesh on CFD

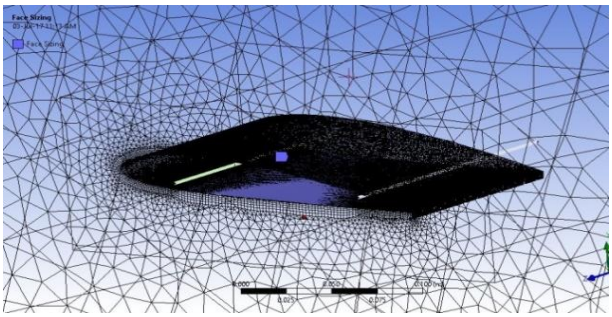

Fig. 05: Mesh generation along airfoil

2.2.4 Convergence Criterion:

In the solver, the convergence criterion was prescribed as the solution reached at a steady state condition where all the residuals are bought to any constant values. For this investigation, the CFD cases were simply set to run a fixed number of iterations.

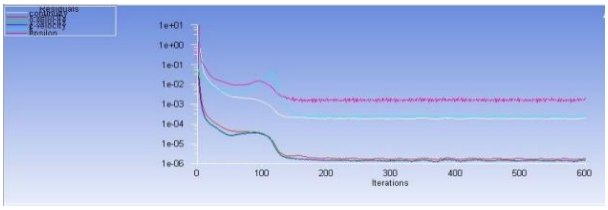

Fig. 06: Residuals converging graph.

2.3 Prototype of the airfoil with flap:

Prototyping of an airfoil body is designed to explore the variation of results by comparing the simulated and experimented outcome. A prototype of NACA 2412 with gurney flap for different height and serrations was built for wind tunnel experiment with the predefined chord length of200mm and span of 120mm. The flaps were made of mild steel and heights were 2% chord (4mm), 3% chord (6mm), 4% chord (8mm) and 5% chord (10mm). The serrations were made with depth and width of 0.01C (2mm). The prototype fabricated in workshop was not as precise as wished for. (Figure 07)

2.4 Wind Tunnel Experiment:

Wind tunnel testing is an effective approach to visualizing what is happening to the flow and surrounding conditions. The experimental investigation was conducted in the wind tunnel of Chittagong University of Engineering & Technology. The wind tunnel is made in the shape of a converging-diverging nozzle to obtain the required flow manipulation and a working section where the model was mounted for the test. In this study, the free stream velocity was 5 m/s which yield the Reynolds number of 68,474 based on the centerline chord of the airfoil.

Lift and drag forces were calculated using force balance setup which had two degrees of freedom. Rotation sting was used to rotate the airfoil for setting up the different angle of attack and airspeed was measured by an anemometer. A honeycomb was implemented in front of the test section in the wind tunnel to reduce flow turbulence and maintaining a steady laminar flow during the study.

Fig. 07: Fabricated prototype of NACA 2412 without and with 3% clean flap

Fig. 08: Wind tunnel setup [6]

3. INVESTIGATIONS AND DISCUSSION

For the purpose of CFD validation, the values obtained from CFD analysis of NACA 2412 with square and triangular serration at an angle of attack ranging from 0º to 24º were compared with the experimental results from the wind tunnel data on the airfoil of similar dimensions and profile at the same Reynolds Number.

After completing the CFD analysis of 3D wing with different flap height with serrations for the different angle of attack, a comparison was made with results obtained from wind tunnel experiment on the basis of the values of C_L, C_D and coefficient of lift to drag ratio (C_L/C_D).

(a) Clean flap

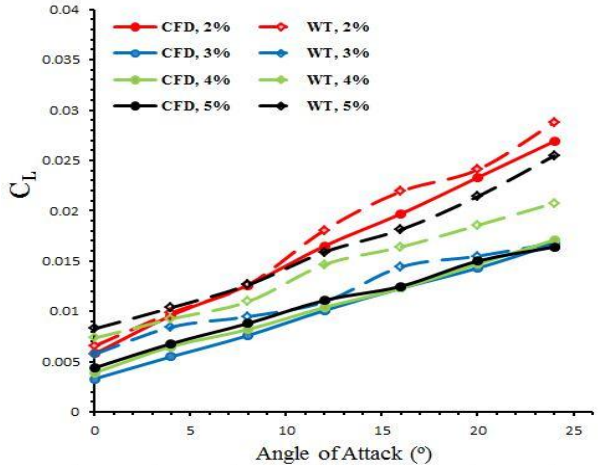

(b) CFD Analysis

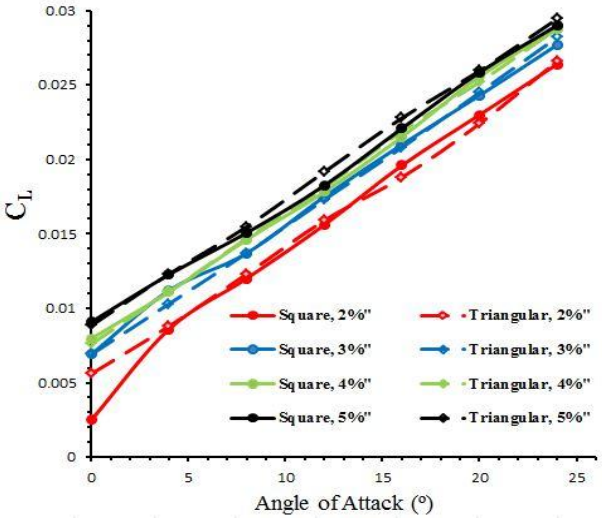

(c) Wind Tunnel Experiment

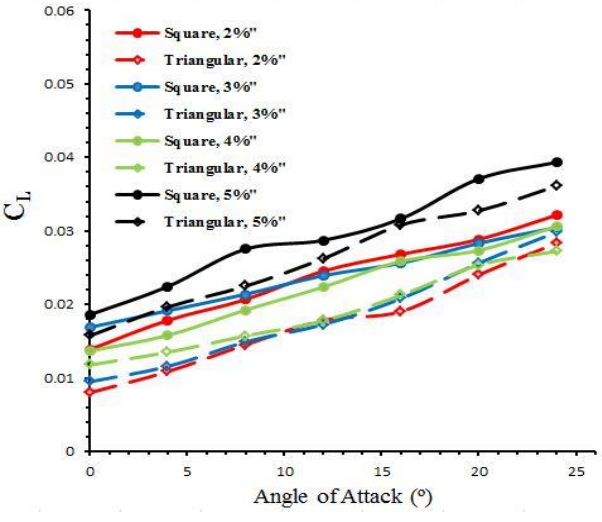

Fig.09: Comparison of lift coefficient for (a) clean flap (b) CFD results for serrations and (c) Wind tunnel experiment

Figure 09 shows the variations of C_L for plain flaps and flaps with square and triangular serration for the different angle of attack. Obviously, an airfoil with plain gurney flap will increase the lift than without gurney flap. This increment in the lift is accompanied by an increase in skin friction drag as shown in figure 10. That means drag is more than a clean wing. 2% and 3% gurney flap increased the maximum lift coefficient by 30.27% and 38.54% respectively. The lift increment is higher with the increment of flap height as well as drag force. The 2% gurney flap proved to be better among others as it has the maximum lift coefficient and minimum drag for this study.

Figure 11 shows the variation of the ratio of lift and drag coefficient as a function of the angle of attack. The increase of maximum C_L/C_D is 17.2%, 41.32%, 62.12% and 65.01% for 2, 3, 4, 5% gurney flap without serration. The increment in the lift to drag ratio was gradually reduced with increment in lift coefficient which means serrated flap is much more effective than clean flap. The square serration increased the lift to drag ratio by 22.39% and the triangular serration increased 14.73%.

Comparison of drag coefficient produced by adding gurney flap was represented by figure 12. The gurney flap increases drag force wherever it is mounted for both serrations. The drag increments are drastic in case of 3, 4 and 5% flap and thereby lift to drag ratio decreases. The drag force sharply increases in case of a small angle of attack and significantly changes before the stall. The fluctuation of results was very high as it was difficult to ensure the dimensional accuracy, laminar flow over the airfoil etc.

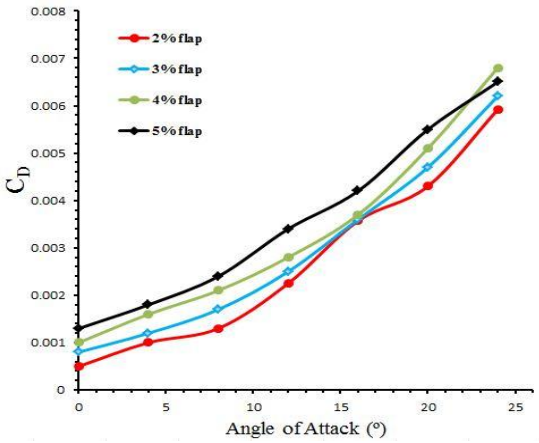

Fig.10: Comparison of C_D for different flap height

After reviewing all the results from the investigation, it can be clearly said that the gurney flap with 5%C height produces maximum lift but increased drag made that inefficient. Flap with 2%C height provided the best performance in these conditions. Serrations were made to increase the effectiveness of the flap. Square serration with 2% flap provided the best configuration of all the serrated flaps by maximizing the lift to drag ratio and remarkable reduction in drag coefficient.

However, as the serration shape and depth changes the flow behavior and thereby gives an opportunity to manipulate the flow field, further in-depth investigations are needed to explore the best combination of serration geometry and gurney flap with a slight change in height. It is also desirable to study the flow separation property change with respect to flap height change.

(a) Clean flap

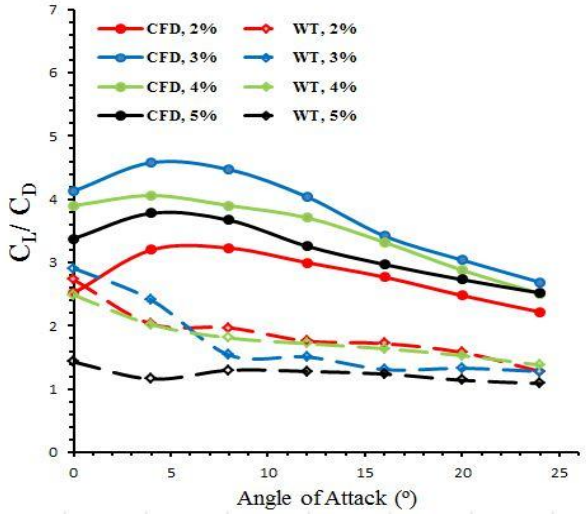

(b) Square serrated flap

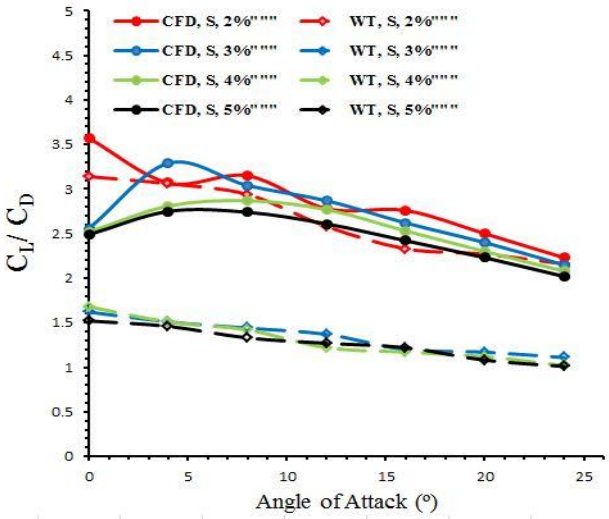

(c) Triangular serrated flap

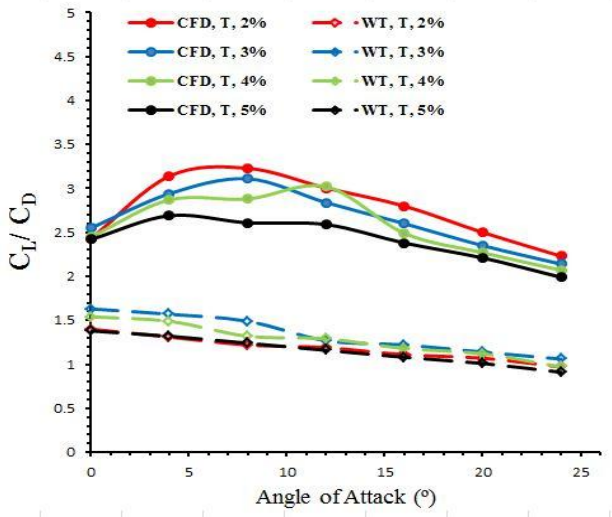

Fig.11: Comparison of lift to drag ratio for (a) clean flap (b) Square serrated flap (c) Triangular serrated flap

(a) Clean flap

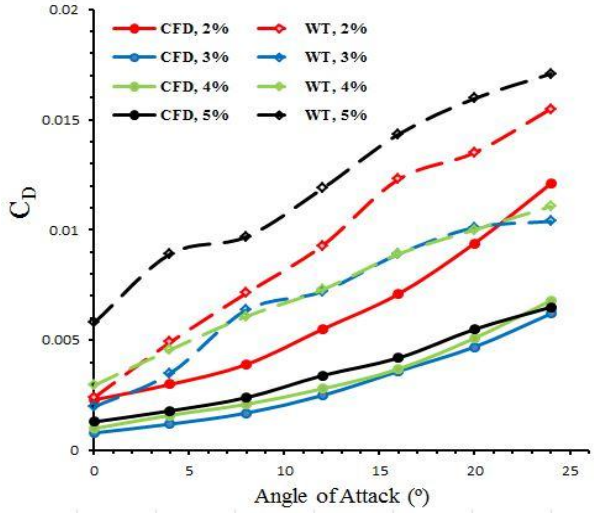

(b) Square serrated flap

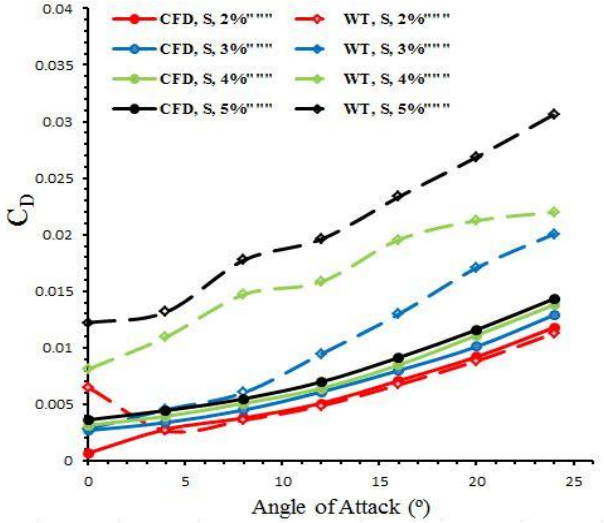

(c) Triangular serrated flap

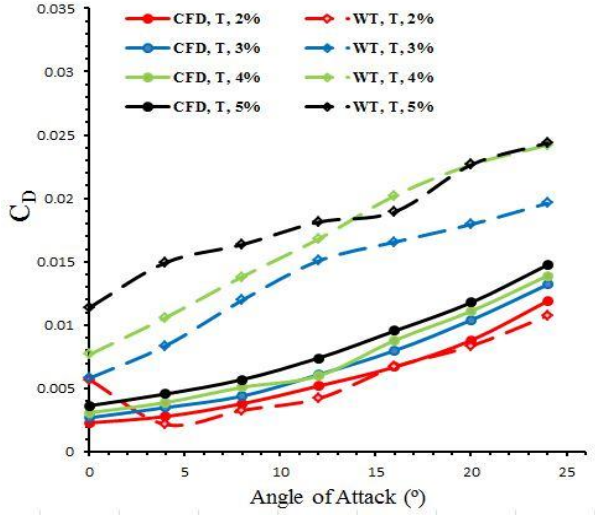

Fig.12: Comparison of drag coefficient for (a) clean flap (b) Square serrated flap (c) Triangular serrated flap

(a) Pressure distribution

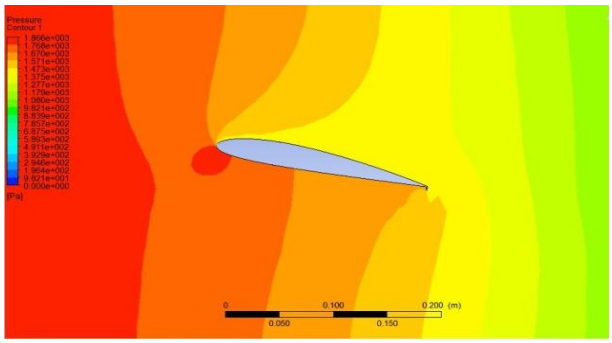

(b) Velocity Distribution

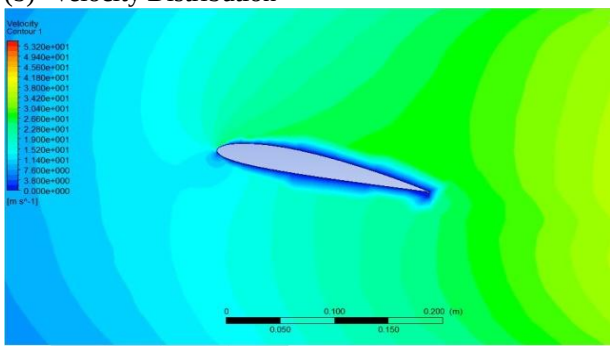

Fig.13: Contour plot for 2% gurney flap at 12º angle of attack (a) Pressure distribution (b) Velocity distribution

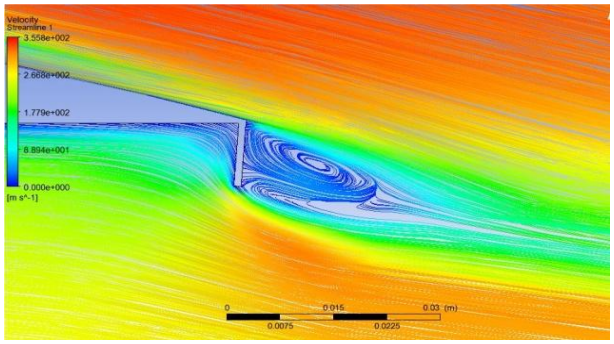

Fig.14: Formation of two contrarotating vortices at angle of attack 4º

5. CONCLUSION

In recent years there has been an increased interest in primary criteria in the design of wings include maximizing efficiency and control; thus increasing desired effects while diminishing undesired effects such as drag so that the wing becomes more functional and provides sufficient means of control. From the study, it is determined that the addition of gurney flap increase the angle of attack before stall which is nearly 15-17 degree for NACA 2412. The wind tunnel and CFD analysis confirmed that the square serration for 2% flap provides the best performance among all as a result of remaining the flap within the boundary layer thickness. Larger gurney flap provides increased lift accompanied with drag increment. The study reveals that the lift to drag ratio is higher for square serration than triangular serration and the factor affecting the performance is the effective area of the flap.

6. SCOPES FOR FUTURE WORKS

Relying on the current research investigations carried on gurney flap, the following recommendations can be made.

- It is undeniable that there is a demand of in-depth knowledge of serrations geometry by which the flow behavior will favorably affect the boundary layer and delay the separation.
- Apart from the square, triangular or hemisphere shaped serration, 'convergent-divergent' grooves can be implemented on the gurney flap.
- A combination of gurney flap and vortex generators can be studied as a passive flow separation control strategy and flow visualization technique can be applied to investigate the streamwise formation of contra rotating vortices behind the flap.

7. REFERENCES

[1] Greg F. Altmann "An investigative study of Gurney flap on a NACA 00036 airfoil" Master Thesis presented to the Faculty of California Polytechnic State University, San Luis Obispo, March 2011

[2] Gai, S. L. and Palfrey R., "Influence of Trailing-Edge Flow Control on Airfoil Performance," Journal of Aircraft, Vol. 40, No. 2, 2003, page 332-337.

[3] Liebeck RH, "Design of subsonic airfoils for high lift," Journal of Aircraft 1978; 15(9): page 547—561.

[4] http://m-selig.ae.illinois.edu/ads/afplots/naca2412.gif

[5] Standard k-epsilon model -CFD-Wiki, the free CFD reference.

[6] ICMERE-2015 PI-273

8. NOMENCLATURE

Symbol	Meaning	Unit
C	Chord length	m
V	Velocity of air	m/s
L	Lift force	N
D	Drag force	N
C_D	Drag coefficient	Dimensionless
C_L	Lift coefficient	---
AOA	Angle of attack	Degree
K	Turbulent kinetic energy	J
ϵ	Turbulent dissipation	m^2/S^3